Wind Farm Transformer Protection Against Lightning Transients Using Air Core Reactor and Resistor

Amir Heidary, Behzad Behdani, Mohamad Ghaffarian Niasar, Marjan Popov

***Abstract*— Integrating renewable energy resources such as wind farms is an increasingly prominent trend for future power grids. However, the wind generator tower is consistently at risk of lightning strikes, putting the wind farms' transformer at risk of damage by lightning transients traveling through the system. Various harmonic contents of the lightning transient can excite the transformer's resonance frequencies, resulting in both terminal and internal overvoltages (OVs). To effectively safeguard transformers against resonance OVs, it is imperative to first identify the resonance points of the transformer. Following this, a protective method must be implemented to mitigate harmonic content magnitudes that contribute to resonance. This paper introduces a series-protection device comprising an air core reactor and suppressor resistance designed to protect the transformer. The research aims to provide solutions to safeguard wind farm transformers from both terminal and internal resonance OVs caused by lightning transients. The effectiveness of the protection device is assessed through analysis, simulation, and experiments conducted in a high-voltage laboratory setup.**

Keywords—Lightning, Overvoltage (OV), Resonance, Surge Protection, Transformers, Transients.

I. INTRODUCTION

Addressing global warming concerns requires a significant shift in the energy sector, particularly through the energy transition [1]. This transition involves moving away from traditional fuel-based power plants towards renewable energy sources (RESs), a trend driven by the need to tackle environmental challenges [2]. Among these RESs, wind energy generators play a crucial role, as they can supply a substantial portion of the energy required by industries [3].

However, the integration of wind energy generators introduces an increased risk of lightning strikes due to their tall towers and sharp edges [4]. A lightning strike on the tower can cause damage to various parts of the power system, including wind generator insulation, converters, cables, and transformers [5]. Lightning-induced overvoltages (OVs) can propagate high-frequency currents throughout the power system [6]. These high-voltages and high-frequency currents impact transformers, and can trigger resonance frequencies within these critical devices [7]. As a result, transformers experience terminal and internal OVs, leading to potential failures [8]. Therefore, wind farm transformers are at a higher risk of resonance OVs and require appropriate protection against transient signals [9].

To protect transformers from transient components caused by lightning and switching events, several protection devices have been proposed [10]. Among these, the surge arrester is the most widely used, as it is directly connected to transformer terminals to mitigate OVs and reduce their magnitude [11]. However, its limitation lies in only providing protection against terminal OVs, allowing high-frequency transients to pass through, potentially leaving internal resonance OVs unchecked [12]. Other protection devices include surge capacitors, R-C snubbers, and zinc-oxide snubbers, all of which utilize shunt capacitor filters [13]. However, these solutions face challenges in their design suitability for transmission voltage levels above 30 kV [14]. Additionally, there are series-connected inductive components [15] work as protection devices such as frequency-dependent devices (FDDs) and chokes [16]. FDDs typically consist of a coil with a specialized ferromagnetic covering [17], while chokes feature a toroidal ferromagnetic ring core with a resistor in the secondary circuit [18] and [19]. Both methods, however, must address the challenge of avoiding saturation of the ferromagnetic material [20].

This manuscript presents a method depicting a parallel air-core inductor and resistor (PAIR) connected in series with the wind farm transformer. The operation of this transformer protection device is thoroughly analysed, and the results are validated through EMTP and FEM simulations, followed by testing conducted in a high-voltage laboratory. The analysis demonstrates that the proposed protection device effectively attenuates harmonic contents that could potentially cause resonance in lightning transient signals without the risk of saturation issues.

The paper is organized as follows: Section II defines the problem and outlines the specifications of the protection device. Section III introduces a protection model for the transformer, while Section IV examines the effects of the protection device. Section V details the experimental test procedure. Finally, Section VII concludes the paper.

This work was financially supported by the Nederlandse Organisatie voor Wetenschappelijk Onderzoek (NWO) in collaboration with TSO TenneT, DSO Alliander, Royal Smit Transformers, and TSO National Grid, UK in the framework of the NWO-TTW project "Protection of Future Power System Components, No.18.699.

The authors are with the Faculty of Electrical Engineering, Mathematics and Computer Science, Delft University of Technology, 2628 CD Delft, The Netherlands (email: A.Heidary@tudelft.nl; B.Behdani-1@tudelft.nl; M.Ghaffarianniasar@tudelft.nl; M.Popov@tudelft.nl)

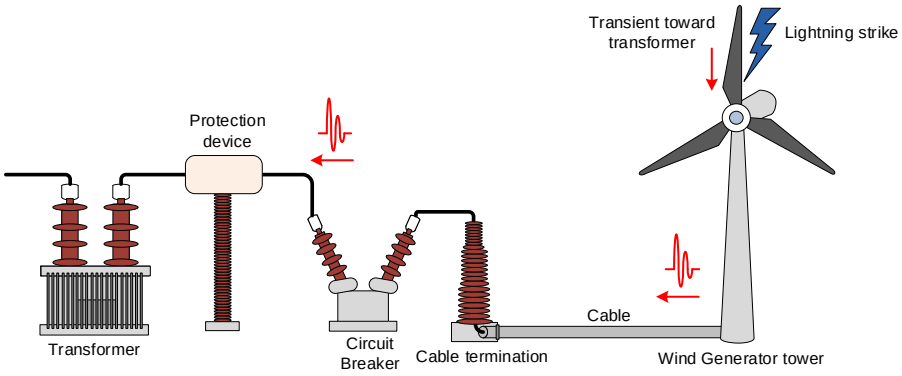

Fig. 1. Diagram of the studied power system.

II. Problem Definition and Solution

The diagram depicted in Fig. 1 illustrates the system under examination, which includes a wind energy generator, a cable, a circuit breaker, a series-protection PAIR device, and a transformer. When lightning strikes the wind turbine, the transient signal travels through the generator and reaches the power cable. As the transient signal, in the form of an electromagnetic wave, moves along the cable, it reaches the cable termination, passes through the circuit breaker, and ultimately arrives at the transformer. This transient signal typically has two key characteristics: a high magnitude and a broad range of harmonic content. As a result, the incoming transient signal can easily cause a resonance overvoltage (OV) in the transformer, which may occur between the transformer winding disks or at the transformer terminals.

To simplify the power system illustrated in Fig. 1, the section from the wind generator to the circuit breaker can be replaced with an equivalent circuit. This part of the system is considered the source of transient signals that can excite resonances from the perspective of both the transformer and the protective device. The simplified electrical system is shown in Fig. 2. The equivalent circuit consists of a current source representing the lightning (i_t) and an RLC equivalent impedance (Zeq).

Additionally, Fig. 3 (a) presents the protection PAIR device. This device includes an air-core inductor and a parallel resistor connected in series with the transformer. The device is isolated from the ground and installed on an isolation stand. The operating principle of the PAIR device is to suppress the magnitude of high-frequency components of the transient signal through the resistive branch. As a result, the PAIR device operates in two modes: at system frequency and above system frequency.

The PAIR device is modelled as a very small inductive impedance in parallel with a relatively large resistor within the system. As a result, power frequency current components predominantly flow through the air-core inductor, causing minimal voltage drop and power loss in that branch. This operational aspect is illustrated in Fig. 3 (b).

$$V_p = I_s\left(R_p + j\omega L_p\right) \tag{1}$$

$$P_{loss} = \frac{(I_s . j\omega L_p)^2}{R_p} \tag{2}$$

Equation (1) defines the PAIR voltage drop V_p during normal operation, which depends on the line current I_s and the air-core inductor impedance (R_p+ωL_p). Equation (2) defines the corresponding small power loss P_{loss} during normal operation.

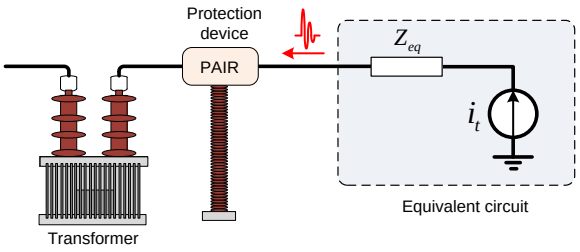

Fig. 2. Simplified diagram of the studied power system.

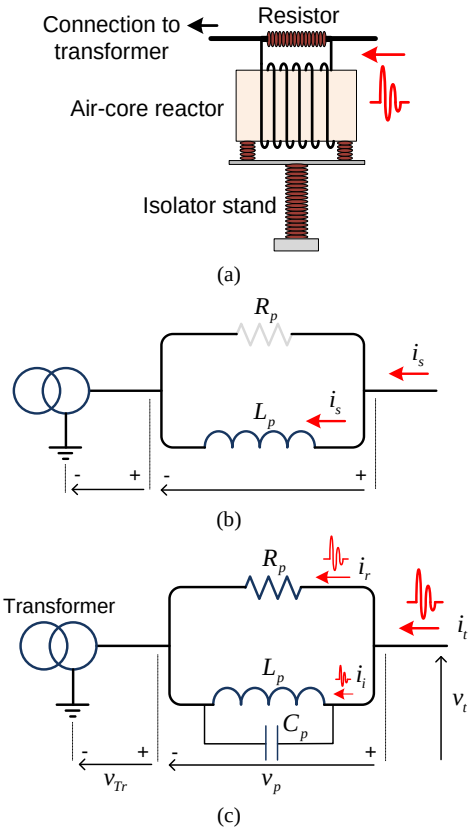

Fig. 3. (a) Topology of the series-protection device, (b) circuit model in grid frequency, (c) circuit model against transient.

In response to transient signals, the PAIR device behaves as a large impedance. In this operational mode, the impedance of the air-core inductor increases due to the high-frequency content of the transient signal, causing most of the current to flow into the resistor branch, effectively suppressing the high-frequency transients.

TABLE I. SPECIFICATIONS OF THE TEST TRANSFORMER.

Parameter	Value
Ratio	10 kV / 0.4 kV
Vector Group	YNyn0
Nominal Power	315 kVA
Nominal Frequency	50 Hz

Additionally, the internal capacitance of the inductor C_p or an external tuning capacitance further increases the impedance of the inductor near the resonance point. This operation is depicted in Fig. 3 (c). Based on this figure, and applying Kirchhoff's Current Law (KCL) to the transient signal passing through the PAIR, equations (3) and (4) can be derived as follows:

$$i_t(t) = i_r(t) + i_i(t) \tag{3}$$

$$i_t(t) = \left(v_p(t)/R_p\right) + \left(1/L_p \int v_p(t)dt\right) + \left(C_p\, dv_p(t)/dt\right) \tag{4}$$

In addition, the voltage at the transformer terminals during the transient is computed by equation (5).

$$v_{Tr}(t) = v_t(t) - v_p(t) \tag{5}$$

Next, by considering the resonance frequency contents of the transient signal that can potentially cause resonance OVs, the voltage of transformer V_{Tr} is calculated in resonance frequency as (6) based on phasor analysis, where ω_r corresponds to the angular frequency of the resonance point.

$$V_{Tr(\omega_r)} = V_{t(\omega_r)} - V_{p(\omega_r)} \tag{6}$$

Following (6), the voltage drop of the PAIR, V_p, in the resonance point is calculated by (7).

$$V_{p(\omega_r)} = I_{r(\omega_r)}.R_p = I_{i(\omega_r)}.\left(\frac{j(L_p/C_p)}{1-\omega^2 L_p C_p}\right) \tag{7}$$

III. TRANSFORMER PROTECTION MODELING

The operational principle of the proposed PAIR-based overvoltage (OV) protection strategy is to mitigate transient surges entering the transformer at its terminals. Achieving this requires a comprehensive model that accurately captures the transformer's frequency-dependent behaviour from the PAIR device's perspective. In this context, a black-box model is constructed for an actual power transformer. This modelling serves two main purposes. First, implementing a high-voltage impulse test in the laboratory poses a risk to the real transformer due to potential overvoltage and resonances. To avoid these risks, the obtained model is used to create a simplified protection laboratory circuit for the transformer. Second, accurately tuning the PAIR device to provide maximum impedance at the transformer's resonance point requires an accurate transformer model. The specifications of the test transformer are provided in Table I.

To begin, the harmonic impedance characteristic of the transformer is measured at its terminal using a vector network analyzer (VNA), as illustrated in Fig. 4. In Fig. 4 (a), the transformer impedance (Z) is measured at the high-voltage (HV) terminal while the remaining terminals are left in an open-circuit condition. Fig. 4 (b) shows the laboratory setup used to measure the transformer's terminal impedance.

In the next step, the vector-fitting technique [21] is applied to calculate a rational approximation of $Y(s) = Z^{-1}(s)$ as the corresponding admittance of the terminal under test with respect to the neutral terminal, given by:

$$Y(s) = d + e \cdot s + \sum_{i=1}^{n+m} \frac{c_i}{s - p_i} \tag{8}$$

where d and e are constants c_i and p_i, respectively, denote residues and poles, considering a number of n real- and m complex poles, while $s = j2\pi f$ is the Laplace variable at frequency f. It is worth noting that the passivity of the approximated rational function is ensured according to the method proposed in [22]. Based on the calculated vector-fitting coefficients in (8), an equivalent circuit model can be realized, according to Fig. 5 [23]. The parameter values of the equivalent circuit are obtained by equations (9)-(14).

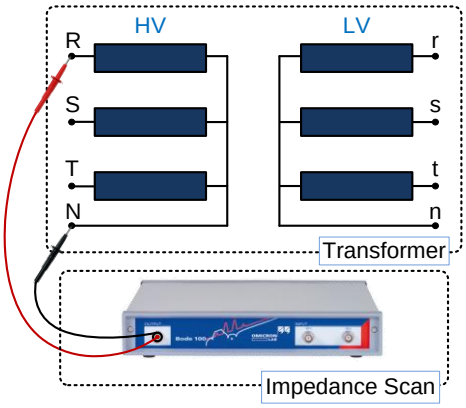

(a)

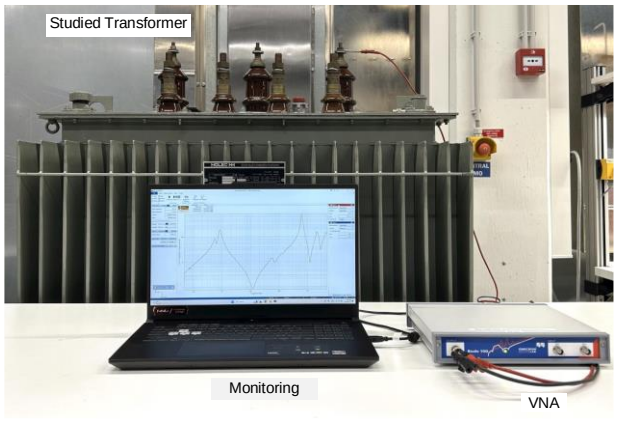

(b)

Fig. 4. Transformer terminal impedance measurement: (a) Schematic representation of the setup, (b) Laboratory setup.

Constants d and e in (8) characterize R_0 and C_0 by:

$$R_0 = 1/d\,, \qquad C_0 = e \tag{9}$$

The real poles characterize the number of n RL branches with $k = 1, \ldots, n$, as:

$$R_k = -p_k / c_k, \qquad L_k = 1/c_k \tag{10}$$

Finally, the complex conjugate pairs with poles $p'_k \pm jp''_k$ and corresponding residues $c'_k \pm jc''_k$ characterise the number of m RLCG branches with $k = n+1, \ldots, m$, yielded by:

$$L_k = 1/2c'_k \tag{11}$$

$$R_k = \left(-2p'_k + 2(c'_k p'_k + c''_k p''_k)L_k\right)L_k \tag{12}$$

$$C_k^{-1} = \left(p'^{\,2}_k + p''^{\,2}_k + 2(c'_k p'_k + c''_k p''_k)R_k\right)L_k \tag{13}$$

$$G_k = -2(c'_k p'_k + c''_k p''_k)C_k L_k \tag{14}$$

Table II summarizes the parameters of the synthesized circuit model shown in Fig. 5, derived from the measured characteristics of the transformer. This circuit model is implemented in EMTP. Fig. 6 compares the measured and simulated transformer terminal impedance characteristics. The simulation is performed for two scenarios: (1) considering all obtained circuit model parameters (including both positive and negative values) and (2) eliminating unimportant parameters to simplify the model. As illustrated, the transformer demonstrates susceptibility to series resonance conditions around 11 kHz.

Given that the primary goal of this study is to propose adequate protection for the transformer against transient surges at its terminals, particular attention is focused on the transformer's resonance frequency. From a surge protection perspective, the equivalent circuit in Fig. 5 can be simplified by retaining only the branches that contribute to resonance while omitting the others. A laboratory circuit can be constructed to replicate the transformer's behaviour around its resonance frequency, allowing for experimental testing of the proposed PAIR device. This experimental setup is demonstrated in Fig. 7 (a).

To ensure that the behaviour of the implemented circuit closely matches that of the studied transformer, a frequency scan is performed using a VNA device, with the results illustrated in Fig. 7 (b).

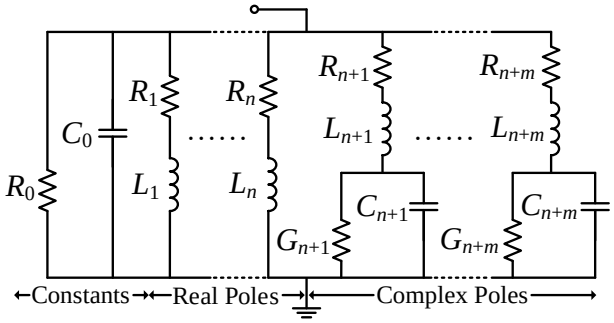

Fig. 5. Synthesized equivalent circuit model.

From the impedance character of the laboratory model synthesized for the transformer, it is evident that the critical resonance of the circuit is at approximately 11 kHz, and its impedance is around 1 kΩ. Accordingly, the synthesized circuit has almost the same character as the studied transformer around the critical resonance point. This circuit will be utilized to evaluate the PAIR in the next step.

TABLE II. SPECIFICATIONS OF THE TEST TRANSFORMER.

Branch k	R_k [Ω]	L_k [mH]	C_k [nF]	$1/G_k$ [Ω]
0	1×10^{6}	-	-	-
1	341.35	11.34×10^{3}	-	-
2	1×10^{5}	107.7	-	-
3	1.6×10^{5}	210×10^{3}	2.97×10^{-1}	-2.63×10^{-7}
4	1.22×10^{3}	53.5	3.25	-8.97×10^{4}
5	-1.41×10^{4}	282.88	1.91×10^{-2}	3.63×10^{5}
6	4.1×10^{3}	4.5	2.44×10^{-3}	-1.12×10^{6}

Implementing a high-voltage impulse test in the laboratory carries risks to a real transformer due to potential overvoltages and resonances. To mitigate these risks, parameters obtained from the real transformer are used to develop a high-voltage laboratory transformer model. This model is designed to closely replicate the behavior of the actual transformer. As can be seen in Table II, using the vector fitting method, several circuit parameters have been obtained with negative values. Auxiliary optimization algorithms have been proposed in the literature to ensure the physical correctness of the equivalent circuit models by calculating non-negative parameters [24]. However, to prevent overcomplicating the analysis, a trial-and-error approach was used in this paper. It was determined that adequate model accuracy around the resonance frequency can be achieved by simply eliminating certain elements from the parameters in Table II. The eliminated elements include all elements in Branch 3, series resistance R5 in Branch 5, and parallel conductance G6 in Branch 6. By comparing the responses of the simplified model with the actual measurements in Fig. 6, it is evident that the corrected model accurately replicates the resonance behavior of the power transformer under study.

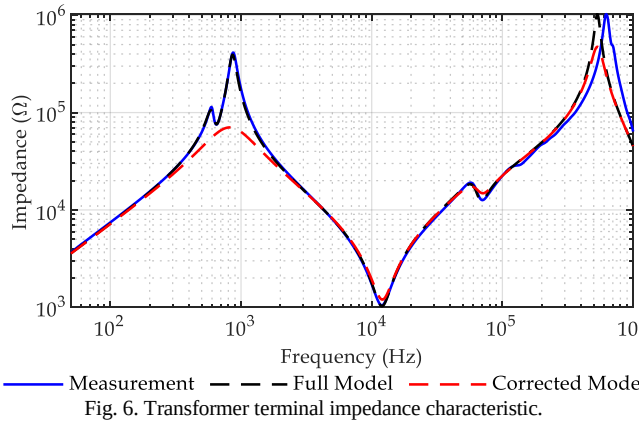

Fig. 6. Transformer terminal impedance characteristic.

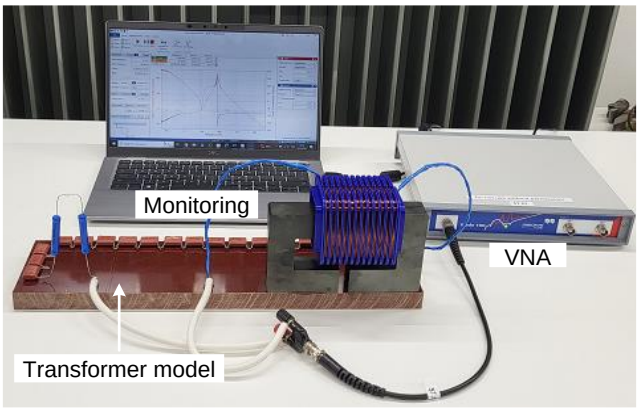

(a)

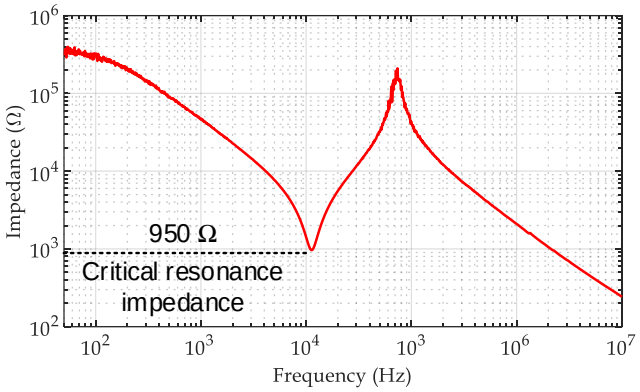

(b)

Fig. 7. (a) laboratory implemented transformer model, (b) the transformer modeled circuit impedance sweep.

To further elaborate on resonance frequency detection and modeling for the development of a protection PAIR, cable-transformer combination presents another critical concern in modern power systems [25]. Similar to standalone transformers, the resonance frequency of a cable-transformer system can be identified through a frequency scan of the cable-integrated transformer. Once the resonance frequency is identified, an air-core reactor with two tuning capacitors can be designed to counteract both critical resonance frequencies. The main steps for both cases follow a similar approach.

IV. Protection Device Evaluation

In this section, the performance of the proposed PAIR is evaluated in three stages. Firstly, the impedance characteristics of the PAIR are analysed using frequency sweep measurements conducted with a VNA device to understand its behaviour in the frequency domain. Next, the configuration shown in Fig. 2 is modelled in EMTP software to determine the transformer's voltage response to a lightning impulse at its terminal. Finally, the PAIR's performance is validated in a high-voltage laboratory setup, where its effectiveness in protecting the transformer circuit is assessed. The results of the EMTP simulations and high-voltage laboratory tests are then compared to ensure robust validation. The laboratory PAIR data are presented in Table III.

TABLE III. Specifications of the Designed PAIR.

Inductance L_p (mH)	Resistor R_p (Ω)	Coil capacitance C_p (nF)	Tunning capacitance C_t (nF)	Voltage test level V_t (kV)
2	1400	2	8	35

The parameters of the proposed PAIR device are presented in Table III. These specifications ensure that the PAIR introduces significant series impedance at the transformer's resonance point, effectively increasing the transformer's minimal impedance at this frequency to prevent resonance overvoltages (OVs). The designed PAIR, depicted in Fig. 8 (a), is based on this strategy.

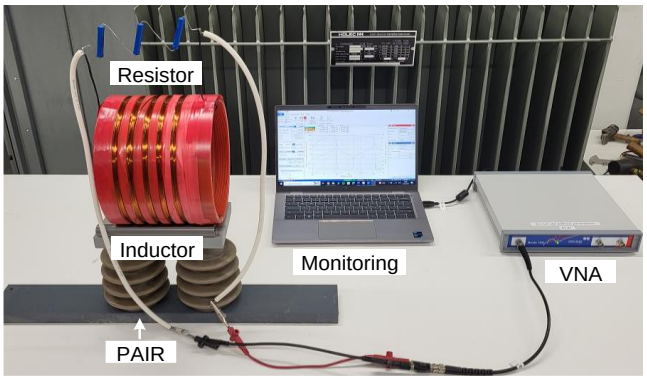

(a)

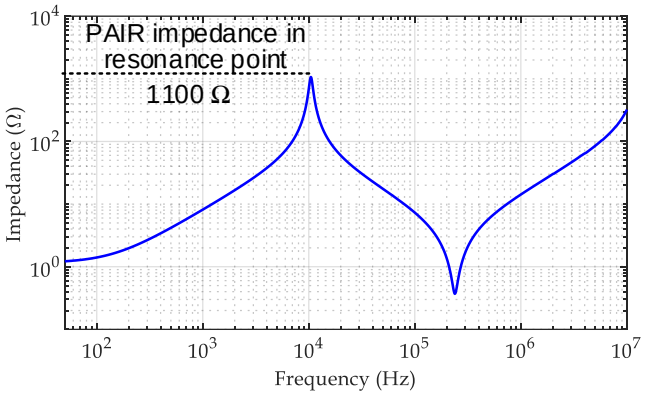

(b)

Fig. 8. (a) Transformer protection model circuit, (b) the transformer modelled circuit impedance sweep.

In the initial test, a frequency scan of the PAIR is performed to confirm its impedance behaviour at the transformer resonance point (11 kHz in this case). As shown in Fig. 8 (b), the PAIR exhibits an impedance of approximately 1.1 kΩ at 11 kHz, which slightly exceeds the transformer's impedance at its resonance frequency. According to (7), the PAIR will suppress more than half of the transformer voltage at this frequency.

Subsequently, the transformer model connected in series with the PAIR is simulated using the EMTP to assess the transformer's voltage response during impulse testing. The time-domain test, illustrated in Fig. 9, along with experimental results, validates the PAIR's effectiveness against impulse signals. The simulation results indicate that nearly 1% of the impulse voltage magnitude is mitigated at the transformer terminal, primarily due to the suppression of the frequency content around 11 kHz. Consequently, the transformer experiences no overvoltage during impulse excitation, confirming the PAIR's effectiveness.

V. Experimental Validation

This section elaborates on the high-voltage laboratory setup used to test the proposed PAIR device. The test circuit configuration is illustrated in Fig. 9 (a). In this setup, the output terminal of the impulse generator is connected to one terminal of the PAIR, with the other terminal linked to the protection-modelled circuit of the transformer. The remaining terminal of the transformer is grounded. Additionally, voltage divider measurement devices are connected to the terminals of both the impulse generator and the transformer.

For the test run, the impulse generator is charged to 33 kV, a level considered safe given the insulation's withstand voltage. The impulse is then applied to the test setup, and the resulting voltages, shown in Fig. 9 (b), are recorded using a high-speed oscilloscope. These recorded results are presented in Fig. 10, together with the results from EMTP simulations.

As shown in Fig. 10, the voltage at the transformer terminal is lower than that of the impulse generator. Specifically, Fig. 10 (a) illustrates that during the high-voltage laboratory test, while the impulse generator reaches a peak magnitude of 33 kV, the peak voltage at the transformer terminal remains at 31.5 kV. This observation closely aligns with the results from the EMTP simulations shown in Fig. 10 (b), confirming the accuracy of the transformer terminal voltage prediction.

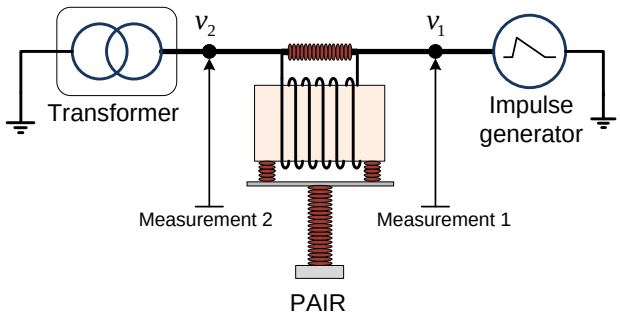

(a)

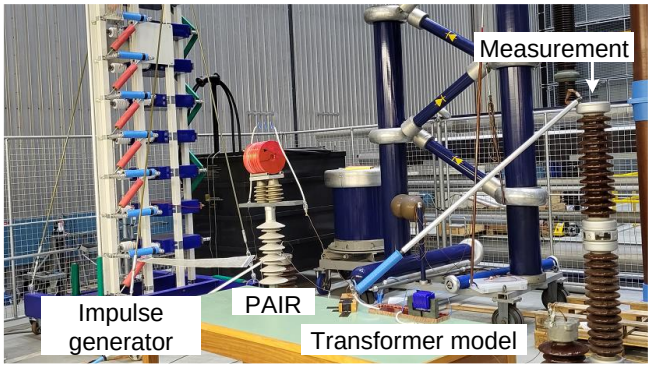

(b)

Fig. 9. (a) Transformer protection model circuit, (b) the transformer modelled circuit impedance sweep.

In summary, the use of the PAIR reduces the voltage at the transformer terminal during impulse testing by 4.5% and effectively prevents overvoltage occurrences due to the transformer's critical resonance point.

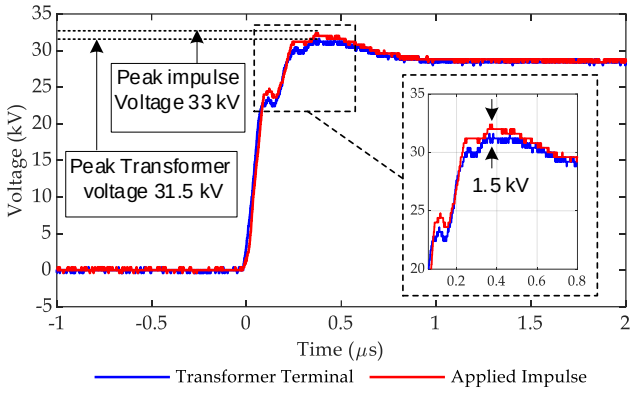

(a)

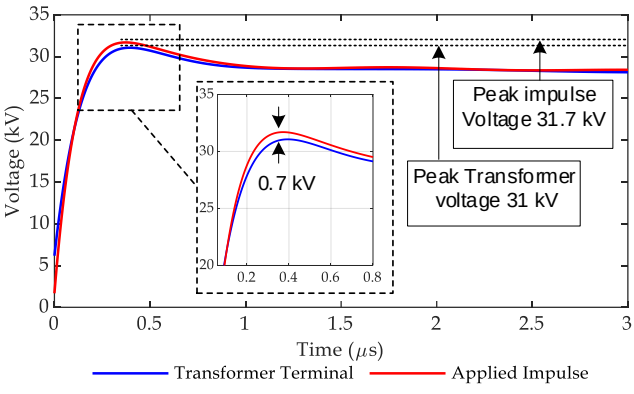

(b)

Fig. 10. Voltage measurement in PAIR impulse test: (a) High-voltage laboratory experimental test, (b) EMTP simulation.

Considering the impedance characteristics of the studied transformer, as shown in Fig. 7 (b), the critical resonance frequency is 11 kHz, which results in a resonance within the transformer. At this frequency, the transformer impedance is minimal (less than 1 kΩ), indicating that harmonics around this frequency can be detrimental. The PAIR is designed to mitigate this by providing high impedance against these harmful harmonics. Consequently, the experimental test focuses on the harmonics received by the transformer within the 9-12 kHz range, both with and without the operation of the PAIR. The results, presented in Fig. 11, provide a clear comparison.

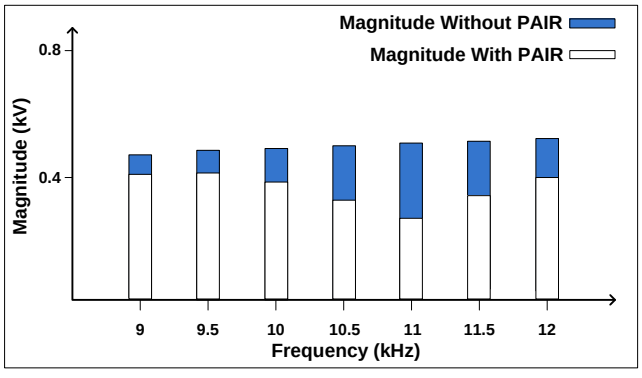

Fig. 11. Transformer Voltage frequency content (9 kHz<f<12 kHz)

As shown in Fig. 11, the magnitude of the frequency content in the transformer voltage is significantly suppressed, indicating that the PAIR effectively limits resonance and overvoltage. Specifically, the frequency content at 11 kHz is reduced by half, demonstrating successful mitigation of resonance at this critical frequency. Additionally, the

frequency content in the range close to 11 kHz is also suppressed, further confirming the PAIR's effectiveness in managing harmful harmonics.

VI. Comparison Study of PAIR

Table IV presents the most significant criteria to highlight the specification of the PAIR over the closest protection concept (choke). These criteria refer to: i) the operation frequency range of each device, ii) the provided impedance against the main frequency of the transient signal in the resonance point, magnetic saturation possibility, and iii) the voltage level.

TABLE IV. Specifications of the test transformer.

Features	PAIR	Choke [17]
Connection type	series	series
Operation frequency range	Tunable in a frequency range	Above 1 MHz
Provided impedance	Above 1 kΩ	Less than 1 kΩ
Saturation possibility	No saturation possibility	Mostly possible
Voltage level	Both the distribution and transmission system	Distribution system

The reasoning behind this claim is that the design of the air-core reactor is applicable across all voltage levels, as presented in Table IV. Therefore, this method is viable for protecting transmission-level transformers that are susceptible to damage from transient phenomena. Additionally, the tuning parallel capacitor and resistor in this method have relatively small values, making them practically implementable.

Based on the data in Table IV, the operating frequency of PAIR is tuneable to align with the resonance frequency of the protected transformer, whereas the choke is not tuneable, as its operating frequency is determined by the fixed R-L circuit components.

Moreover, PAIR's air-core design eliminates concerns about core saturation, a significant issue for core-based series reactors like the choke. In terms of operating voltage levels, PAIR also has an advantage. Its air-core design allows for greater adaptability at higher voltage levels, while the choke, with its compact magnetic core, is typically limited to distribution transformers.

In summary, this comparison demonstrates that PAIR offers several advantages over the traditional choke as a protection method. PAIR not only improves resilience at higher voltage levels but also provides reliable protection against resonance overvoltages in transformers.

VII. Conclusion

This paper focuses on developing a protective device designed to shield wind farm transformers from transient signals that can trigger resonance overvoltages (OVs). The proposed protection device, referred to as PAIR (Parallel Air-core Inductor Resistor), consists of an air-core inductor and a parallel resistor connected in series with the transformer. A comprehensive analysis, including PAIR design, EMTP simulations, frequency sweep measurements, and high-voltage impulse tests, demonstrates that the PAIR effectively safeguards transformers against resonance overvoltages without encountering saturation issues in its inductor. The simulated results and high-voltage impulse tests reveal that not only does the transformer coil avoid reaching overvoltage levels, but its voltage magnitude also decreases by 4.5% during impulse testing. Furthermore, the measurements of the harmonic content around the transformer's resonance point (11 kHz) show a 50% reduction in the magnitude of these harmonics. This successful operation of the PAIR mitigates overvoltage risks and ensures the stable performance of transformer systems in wind farms. Furthermore, this protection method is applicable to all types of transformers, with the only variation being the critical resonance frequency, which determines the specific tuning of the PAIR device.

References

[1] D. Bogdanov, J. Farfan, K. Sadovskaia, A. Aghahosseini, M. Child, A. Gulagi, et al., "Radical transformation pathway towards sustainable electricity via evolutionary steps", *Nature Commun.*, vol. 10, no. 1, pp. 1-16, Dec. 2019.

[2] M. Child, D. Bogdanov, A. Aghahosseini and C. Breyer, "The role of energy prosumers in the transition of the finnish energy system towards 100% renewable energy by 2050", *Futures*, vol. 124, Dec. 2020.

[3] V. Yaramasu, B. Wu, P. C. Sen, S. Kouro and M. Narimani, "High-power wind energy conversion systems: State-of-the-art and emerging technologies," in *Proceedings of the IEEE*, vol. 103, no. 5, pp. 740-788, May 2015.

[4] A. Candela Garolera, K. L. Cummins, S. F. Madsen, J. Holboell and J. D. Myers, "Multiple Lightning Discharges in Wind Turbines Associated With Nearby Cloud-to-Ground Lightning," in *IEEE Transactions on Sustainable Energy*, vol. 6, no. 2, pp. 526-533, April 2015.

[5] A. Candela Garolera, S. F. Madsen, M. Nissim, J. D. Myers and J. Holboell, "Lightning Damage to Wind Turbine Blades From Wind Farms in the U.S.," in *IEEE Transactions on Power Delivery*, vol. 31, no. 3, pp. 1043-1049, June 2016.

[6] A. Andreotti, A. Pierno and V. A. Rakov, "A New Tool for Calculation of Lightning-Induced Voltages in Power Systems—Part I: Development of Circuit Model," *IEEE Transactions on Power Delivery*, vol. 30, no. 1, pp. 326-333, Feb. 2015.

[7] S. Visacro, "Recent Advances in Lightning Research and Their Impact on the Protection of Electric Systems," *2018 34th International Conference on Lightning Protection (ICLP)*, Rzeszow, Poland, 2018, pp. 1-4.

[8] W. Yuanfang, and C. Zhou, "Experimental studies on the use of MOV in transformer windings inner protection," in *IEEE Transactions on Power Delivery*, vol. 20, no. 2, pp. 1441-1446, April 2005.

[9] M. Hori et al., "Internal winding failure due to resonance overvoltage in distribution transformer caused by winter lightning," in *IEEE Transactions on Power Delivery*, vol. 21, no. 3, pp. 1600-1606, July 2006.

[10] S. Ghasemi, M. Allahbakhshi, B. Behdani, M. Tajdinian, and M. Popov, "Probabilistic analysis of switching transients due to vacuum circuit breaker operation on wind turbine step-up transformers," in *Electric Power Syst. Res.*, vol. 182, no. 106204, p. 106204, 2020, doi: 10.1016/j.epsr.2020.106204.

[11] A. Heidary, M. G. Niasar, M. Popov and A. Lekić, “Transformer Resonance: Reasons, Modeling Approaches, Solutions,” *IEEE Access*, vol. 11, pp. 58692-58704, 2023.

[12] M. Hori, M. Nishioka, Y. Ikeda, K. Noguchi, K. Kajimura, T. Kawamura “Internal winding failure due to resonance overvoltage in distribution transformer caused by winter lightning,” *IEEE Transactions on Power Delivery*, vol. 21, no. 3, pp. 1600-1606, July 2006.

[13] M. A. Atefi, M. Sanaye-Pasand and S. Bahari, “Preventing Transformer Energizing Resonant Overvoltages Using Surge Arrester Temperature Rise Index and Controlled Closing Method,” *IEEE Transactions on Power Delivery*, vol. 28, no. 2, pp. 998-1006, April 2013.

[14] P. E. Sutherland, “Snubber Circuit Design for Transformers in an Urban High Rise Office Building,” *IEEE Transactions on Industry Applications*, vol. 51, no. 6, pp. 4347-4356, Nov.-Dec. 2015.

[15] A. Heidary, M. Ghaffarian Niasar, and M. Popov, The principle of magnetic flux switch. Scientific Reports, vol. 14, no. 1, pp. 8990, 2024.

[16] F. Nasirpour, Amir Heidary, M. G. Niasar “High-frequency transformer winding model with adequate protection”, *Electric Power Systems Research*, vol. 223, 2023.

[17] S. M. Korobeynikov, S. I. Krivosheev, S. G. Magazinov, V. A. Loman and N. Ya, “Suppression of Incoming High-Frequency Overvoltage in Transformer Coils,” *IEEE Transactions on Power Delivery*, vol. 36, no. 5, pp. 2988-2994, Oct. 2021.

[18] D. Smugała, Wojciech Piasecki, Magdalena Ostrogórska, Marek Florkowski, Marek Fulczyk, Ole Granhaug “New approach to protecting transformers against high-frequency transients–wind turbine case study,” *Prz. Elektrotech*, vol. 89, pp.186-190, 2013.

[19] A. Heidary, M. G. Niasar and M. Popov, "Comprehensive Evaluation of Toroid Ring Core Parallel Inductor and Resistor as a Transformer Protection Device," *IEEE Transactions on Circuits and Systems I*: Regular Papers, doi: 10.1109/TCSI.2024.3428363.

[20] A. Heidary, M. G. Niasar, M. Popov, “Series magnetic coupled reactor saturation considerations for high voltage AC and DC power systems”, *International Journal of Electrical Power & Energy Systems*, vol. 158, 2024.

[21] B. Gustavsen and A. Semlyen, “Rational approximation of frequency domain responses by vector fitting,” *IEEE Transactions on Power Delivery*, vol. 14, no. 3, pp. 1052-1061, July 1999, doi: 10.1109/61.772353.

[22] B. Gustavsen, “Passivity Enforcement of Rational Models via Modal Perturbation,” *IEEE Transactions on Power Delivery*, vol. 23, no. 2, pp. 768-775, April 2008, doi: 10.1109/TPWRD.2008.916764.

[23] G. Antonini, “SPICE equivalent circuits of frequency-domain responses,” *IEEE Transactions on Electromagnetic Compatibility*, vol. 45, no. 3, pp. 502-512, Aug. 2003, doi: 10.1109/TEMC.2003.815528.

[24] I. Rahimi Pordanjani, C. Y. Chung, H. Erfanian Mazin and W. Xu, "A Method to Construct Equivalent Circuit Model From Frequency Responses With Guaranteed Passivity," in IEEE Transactions on Power Delivery, vol. 26, no. 1, pp. 400-409, Jan. 2011.

[25] B. Behdani, M. Ghaffarian and M. Popov, "Analysis of Cable-Transformer Resonant Interactions Due to CB Prestriking Transients," 2024 IEEE International Conference on Environment and Electrical Engineering and 2024 IEEE Industrial and Commercial Power Systems Europe (EEEIC / I&CPS Europe), Rome, Italy, 2024, pp. 1-6, doi: 10.1109/EEEIC/ICPSEurope61470.2024.10751644.